RESEARCH ARTICLE

VOLCANICA

Numerical modeling predicts seismic resonances in the magma chamber-conduit system due to wavefield capturing

Fabian Limberger*[α,γ] and Georg Rümpker†[α,β]

[α] Institute of Geosciences, Goethe-University Frankfurt, 60438 Frankfurt am Main, Germany.
[β] Frankfurt Institute for Advanced Studies, 60438 Frankfurt am Main, Germany.
[γ] Institute for Geothermal Resource Management, 55411 Bingen, Germany.

Submitted: 2024-01-31 | Accepted: 2024-05-21 | Published: 2024-07-18

Editor: C. Montagna | Typesetter: J. Farquharson

Abstract

This study utilizes 3D numerical models to simulate seismic resonances in a volcanic edifice, arising from the interaction between an externally excited wavefield and a magma chamber-conduit system. The magma chamber and conduit efficiently capture the incident wavefield of both P- and S-waves, excited by a high-frequency (~10 Hz) earthquake located within the edifice. Due to multiple internal reflections off the boundaries of the chamber and conduit, prolonged reverberations occur, which are guided along the conduit. Temporal and spectral analyses of synthetic seismograms illustrate that models with larger chambers and wider conduits consistently yield larger resonance amplitudes at distinct frequencies. Our models indicate that a larger magma chamber can produce an intensified scattered wavefield with a broad frequency range, observable up to several hundred meters away from the central conduit. Generally, these externally initiated 'calabash resonances' may appear as tremor-like signals at seismometers on the edifice, accompanying more conventional seismic events in its proximity.

Keywords: Volcano; Earthquake; Edifice; Scattering; Imaging; Modelling.

1 Introduction

The properties of the magmatic plumbing system within the volcanic edifice are fundamental for characterizing volcanoes, enhancing our understanding of eruptive processes, and improving their forecasts. Generally, the interaction and response of seismic wavefields to the internal structure and topography of the volcanic edifice can offer valuable insights into the geometry and physical properties of the volcanic plumbing system [e.g. De Siena et al. 2014; Reiss et al. 2022] as well as on the imaging of heterogeneous velocity distribution [O'Brien et al. 2023]. Seismic signals observed at volcanoes encompass volcano-tectonic events, tremors, resonances, and relatively long-period signals, recorded in various volcanic regions worldwide, e.g. Redoubt, Alaska [Power et al. 1994]; Soufrière Hills, Montserrat [Miller et al. 1998]; Arenal, Costa Rica [Hagerty et al. 2000]; Erebus, Antarctica [Rowe et al. 2000]; Galeras, Colombia [Gómez M and Torres C 1997]; Karymsky, Russia [Johnson and Lees 2000]; Lascar, Chile [Hellweg 2000].

Among the signals described above, volcanic tremors persist over time periods ranging from seconds to hours and days, while typical long and short-period seismic events at volcanoes are more transient [e.g. Muñoz et al. 1990; Nishi et al. 1996; De Barros et al. 2013]. The tremors are thought to result from seismic events induced by magma (or fluid) movements within the volcanic system, which can cause resonances in the magma-filled conduit [Chouet 1986; Ferrazzini and Aki 1987; Chouet 1988; Jousset et al. 2003; Sturton and Neuberg 2003; Neuberg et al. 2006; Sturton and Neuberg 2006]. Liang et al. [2020] conducted a study on very long-period seismic signals and resonances in a conduit-crack system connected to a reservoir. They used oscillating magma as a source, which causes surface displacements through crack inflation and deflation. The presence of multiphase flow in the magma and stratification in the conduit can generate acoustic-gravity waves, complicating the analysis of resonant signals at volcanos [Karlstrom and Dunham 2016]. Wang et al. [2024] simulated the seismic wavefield radiation resulting from a caldera collapse and the response of the underlying magmatic reservoir to explain the complex seismic signals observed during such collapse events. Jousset et al. [2004] and Sturton and Neuberg [2006] conducted seismic waveform modeling of long-period signals. They demonstrated that the magma-filled conduit acts as a seismic resonator or wave guide due to the contrasting wave speeds between conduit and host rock. Likewise, Cadena and Sánchez [2022] modeled long-period seismic waves observed at Galeras volcano (Colombia) revealing resonances of the seismic signals in the magma-filled conduit. Their studies rely on 2D models with a seismic source situated within the conduit. However, they do not consider the effects due to a magma chamber and an externally generated wavefields, which could result from, e.g. far field seismic sources such as volcano-tectonic events or deep magmatic fracturing [Domínguez et al. 2001; De Barros et al. 2013].

In this study, we focus on modeling the wavefield scattering and resonances of a magma-filled chamber and conduit system. Compared to existing studies, the seismic source is located outside the magmatic system, but inside the edifice. Using synthetic seismograms obtained from 3D modeling that allow the propagation of attenuated P- and S-waves in the host rock and magma, we examine the signals recorded at a receiver line across the volcanic edifice. Seismograms on the surface are linked with wave dynamics in the chamber-conduit system. To more accurately constrain potential sources and processes of wave scattering and reverberations in the volcanic edifice, we systematically vary the

* f.limberger@geophysik.uni-frankfurt.de
† rumpker@geophysik.uni-frankfurt.de

size of the magma chamber and width of the conduit within the models.

The magma chamber used in our model of the volcanic edifice is relatively shallow and small, whereas chambers deeper in the crust are typically larger. With our research, we aim to improve the understanding of the complex seismic resonance response of smaller magmatic structures inside the edifice, which generally might be overlooked by imaging methods, e.g. tomography. Incoming seismic waves from a distant earthquake are characterized by relatively large wavelengths. Contrastingly, local and shallow seismic activity [Patanè et al. 2017], e.g. at the crater or close to shallow magmatic structures (such as a magmatic conduit), produces waves with significantly shorter wavelength. Such waves have the potential to be captured by smaller structures followed by resonances, as investigated in our study. This could be of general advantage concerning imaging techniques applied on shallow objects or minor magmatic structures inside the edifice.

2 Model and setup

We perform simulations of wavefield propagation using the `Salvus` software package, which employs the spectral element method to solve the elasto-dynamic wave equation, taking into account attenuation effects [Afanasiev et al. 2018]. The volcanic edifice considered here has a maximum height of 2000 m (Figure 1). To focus on local and shallow seismic processes within the edifice and to reduce computational costs, we use a cropped modeling range of 800 × 800 m horizontally and 2500 m (from −500 to 2000 m) vertically. The cylindrical conduit, located at the center of the model, has a vertical length of 400 m and a diameter that varies using four different models (D = 20 m, 30 m, 40 m, 50m), extending up to the surface. The modeled magma chamber is relatively shallow (comparable to Stromboli, see Patanè et al. [2017]) and is depicted as a symmetrical sphere connected to the base of the conduit, with varying radii (R = 0 m, 50 m, 100 m, 200 m), while the conduit length remains fixed. Both the chamber and conduit are radially symmetric along the z-axis of the model. A visualization of the increasing chamber size in the model is depicted in Figure 1.

A double-couple source is positioned in the x-z-plane, beneath the chamber at horizontal position x = −200 m and y = 0 m, and vertical position z = 1000 m. The coupled forces of the source are oriented diagonally, rotated by 45° around the y-axis. This source mechanism simulates a typical volcano-tectonic event within the edifice, generating both P- and S-waves. We use a Ricker-wavelet source function with a dominant frequency of 10 Hz, suitable for shallow and local seismic events in the vicinity of the volcano. The physical parameters of the host rock and magma (Figure 1) are based on the values used in existing studies, such as Jousset et al. [2004] and Cadena and Sánchez [2022]. The used elastic parameters are consistent with empirical data and are characteristic for rhyolitic rock [e.g. Christensen and Stanley 2003; Ji et al. 2019] or shallow basalts [Lesage et al. 2018]. We also include attenuation of P- and S-waves within both the host rock (weak damping) and magma (stronger damping). The S-wave velocity in the host rock is fixed to 1500 m s^{-1} and 450 m s^{-1} in the magma, to model partially melted rock [Paulatto et al. 2022]. However, as described below (see section on Effects of reduced S-wave velocity in the magma) the S-wave velocity in the magma is systematically decreased using models with Vs = 750 m s^{-1}, 450 m s^{-1}, 150 m s^{-1}, and Vs = 0 (acoustic medium), to approximate higher melt content.

A receiver line, composed of 800 receivers spaced at 1 m apart, is positioned along the surface across the volcanic edifice. In contrast to previous studies, we assume that the magma is not entirely an acoustic fluid to better approximate the properties of a viscous magmatic mush, allowing for the propagation of S-waves. The mesh consists of hexahedral elements and the discretization adheres to a minimum of three elements per wavelength. The polynomial order (controlling the grid points per element) is set at four, ensuring sufficient resolution of structures and wavefields. Absorbent layers (see Figure 1) of appropriate thickness are attached to the model boundaries to suppress artificial reflections. We obtain synthetic seismograms in units of ground velocity at each of the 800 receivers.

3 Results

3.1 Wavefield capturing and resonance generation

We assume a seismic source located within the edifice (Figure 1). This source, situated beneath the edificial plumbing system (Figure 2A), excites a wavefield that encompasses both P- and S-waves. The wavefield is then captured by the magma chamber and the conduit, both of which have a lower velocity (Figure 2B). Within the simulated magmatic chamber, multiple reflected intersecting wavefronts constructively interfere and lead to resonances. The main mechanism for the resonance generation is the capturing of the wavefield by a drop of the seismic velocity between the host rock and the magma. In addition to these resonances, wavefronts are reflected multiple times off the boundaries of the chamber and conduit, which leads to general reverberations of the signal. These resonances and reverberations can persist for an extended duration of several seconds (Figure 2C and Figure 3D). Some of their energy is also transmitted back into the surrounding rock. Compared to transient signals from earthquakes (P- and S-wave) with a relatively broad spectrum, resonances are typically characterized by prolonged and amplified periodic oscillations at distinct frequencies. This phenomenon is shown in more detail in Figure 3, discussed subsequently.

3.2 Effects of magma chamber size and conduit width

We further explore the influence of the size of the magma chamber and with of the conduit on the resulting resonances within both the chamber and conduit. Seismograms shown in Figure 3A–D and Figure 4A reveal that the resonances undergo significant changes as the size of the magma chamber increases: The separation of P- and S-wave arrivals becomes less clear, and their peak amplitudes (especially after the first S-wave arrivals) become more equal over time. The most pronounced resonances are observed at central stations above and near the 20 m wide conduit (Figure 3). For smaller magma chambers, resonant S-waves impact a range of up to 50 m

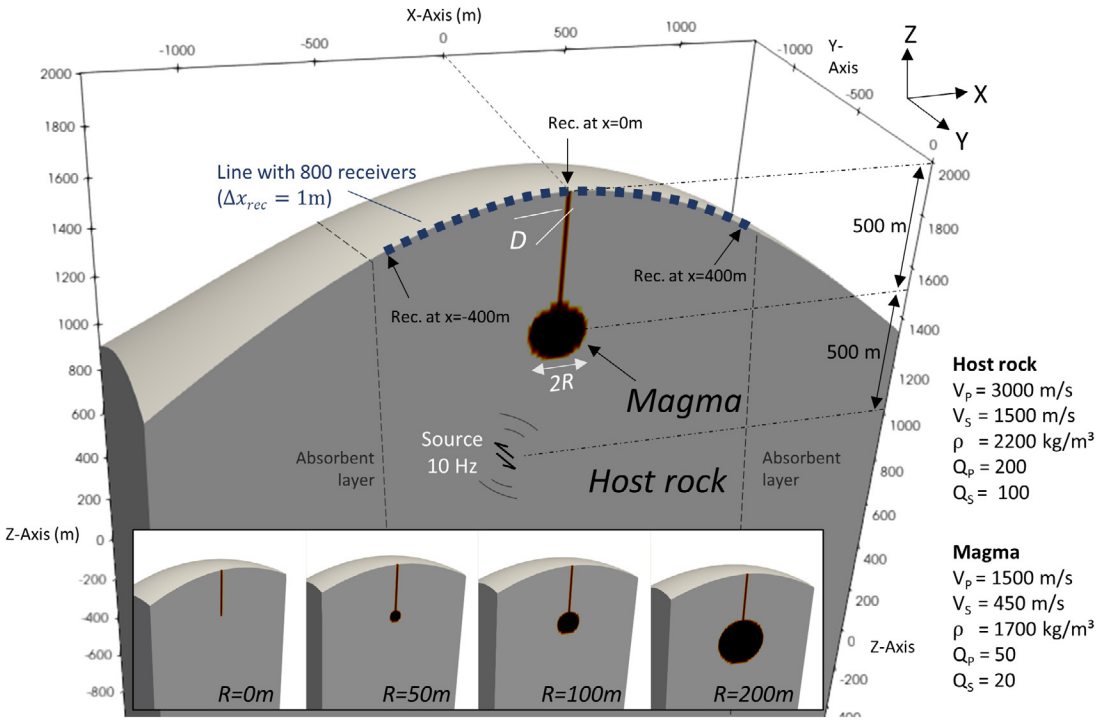

Figure 1: Computational model of the volcano edifice featuring a chamber with varying radius of R = 0 m, 50 m, 100 m, 200 m and a conduit with varying width of D = 20 m, 30 m, 40 m, 50 m. A double-couple source is positioned at (x, y ,z) = (−200, 0, 1000) and is characterized by a 10 Hz Ricker wavelet. The properties of the host rock and magma are similar to those described in Jousset et al. [2004]. except for the (non-zero) VS velocities inside the mushy magmatic system. Absorbent layers are attached to the actual model domain of 800 × 800 × 2500 m, however, the absorbent layers are not depicted in the following figures.

away from the center. This range of impact decreases as the chamber size increases.

Furthermore, the initial P- and S-wavefront are observable across the entire edifice (Figure 3). However, this wavefield becomes significantly more dispersed and scattered for larger simulated magma chambers (as seen in Figure 3D and 4C). Within the conduit itself, waves undergo multiple reflections off its boundaries. This behavior is influenced by both frequency and conduit width. To accurately determine the frequency content of the resonances, we separate the onset of the primary wave (P-wave) before 0.65 s from the subsequent S-wave and other longer-lasting resonances after 0.65 s (see Figure 4). Our analysis confirms that both the chamber size and the width of the conduit influence the S-wave magnitude and dominant frequencies (see Figure 4A–B). Contrarily, it is interesting to note that the frequency content of the P-wave (before 0.65 s) remains largely unaffected, exhibiting only minor variations in response to changes in the sizes of the magma chamber and conduit. The corresponding spectra exhibit a broad-peak amplitude centered at about 18 Hz for small magma chambers with radii up to 50 m. For larger chamber sizes (e.g. 200 m radius), this peak splits up into several narrow peaks with dominant (resonant) frequencies of 16, 18, and 21 Hz (Figure 4A). Irregular splitting of spectral peaks, albeit at lower frequencies, also occurs as the conduit width increases (Figure 4B)—even for smaller chambers. This suggests that relatively low-frequency resonances observed near the conduit result from a wider conduit, while a larger magma chamber tends to broaden the spectrum, also towards higher frequencies.

Based on our results at greater distances from the conduit (Figure 4C), we infer that a significantly intensified scattered wavefield, characterized by a broad frequency range with a distinctly peaked spectrum, is also indicative of a large magma chamber within the edifice. While the primary source frequency is centered at 10 Hz, the recorded resonance frequencies reach up to 23 Hz. This indicates substantial shifts in dominant frequencies, which are mainly related to the conduit, as the effects occur even without a magma chamber (Figure 4A). For instance, with a conduit width of D = 20 m, the frequency spectrum predominantly spans from 13 Hz to 22 Hz. In contrast, a conduit width of D = 50 m exhibits a range between 5 Hz and 16 Hz (Figure 4B).

3.3 Effects of reduced S-wave velocity in the magma

We investigate the impact of a reduced S-wave velocity in the magmatic conduit on the resonances and compare the results to those of an acoustic magma (Figure 5). In case of a relatively high S-wave velocity (Vs = 750 m s^{-1} or 450 m s^{-1}), the onset of the P- and S-wave are distinctly detectable in the seismogram (Figure 5A and B). With decreasing wave velocity in the magma, the resonances show a prolonged duration and the onset of the S-wave is muted or smeared. In case of an acoustic fluid (Figure 5D), the amplitude of the P-wave onset

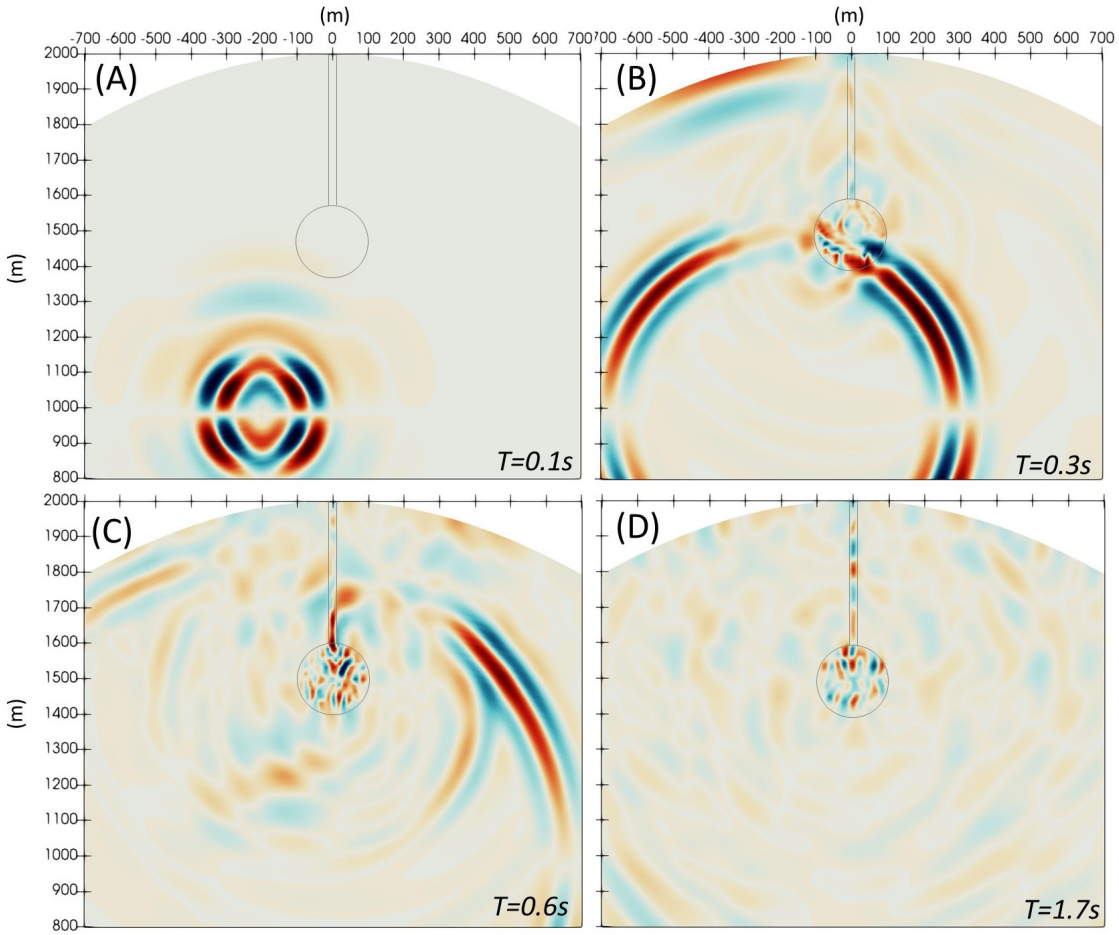

Figure 2: The wavefield (*z*-component) at various time steps, T_i, for the model with a magma chamber radius R = 100 m and conduit width D = 20 m. The vertical axis (horizontal axis) in the figure represents the vertical z-axis (horizontal x-axis) of the model (Figure 1). [A] Excitation of the wavefield at a source within the edifice below the magma chamber. [B] The reduced seismic velocities within the magma chamber and conduit lead to capturing of the incident wavefield. [C] The wavefield within the magma chamber-conduit system reflects at its internal boundaries. [D] The reverberations within the magma chamber-conduit system induce 'calabash resonances', similar to a calabash fruit's shape. The wavefields in [A]–[D] are individually normalized to the maximum amplitude of the wavefield to enhance the visualization of small amplitudes.

is reduced as well, however, resonant signals in the seismogram are significantly prolonged up to a duration of several seconds. These observations imply that pronounced and prolonged resonances, particularly of the S-wave, are indicative for wave velocity characteristics in the magma that could provide rheological information about the magma, which is discussed later. For simplification and reducing numerical costs, the models used in this section neglect the magma chamber and are two-dimensional (see details in Supplementary Material 1 Figure S4).

3.4 Effects of a far-field plane wavefield

We model an incoming plane P-wave (Ricker wavelet) from the bottom of the model to account for possible interactions of the magma chamber with waves from a more distant earthquake. We chose a dominant frequency of the plane wave of 2 Hz and 10 Hz, to examine frequency-dependent behavior (Figure 6). We find that the wave-capturing process is wavelength-dependent. In case of a 10 Hz wave (Figure 6D), resonances are clearly observable in the center of the seismic profile, however, in case of a 2 Hz wave (Figure 6C), the resonances are negligible. This implies that lower-frequency regional and teleseismic wavefields have only limited interaction with a local magma chamber-conduit system, reducing the chance of detecting resonance signals at the surface that are generated by a wave-field capturing process. This highlights the importance of taking local seismic activity into account.

4 Discussion

The results underscore the significance of resonances within the magma chamber and conduit system, triggered by seismic waves excited by an external source. Unlike previous studies that utilized 2D models and considered seismic events within a conduit without magma chamber [e.g. Jousset et al. 2004; Sturton and Neuberg 2006; Cadena and Sánchez 2022], we have conducted simulations in 3D that incorporate both a conduit and a magma chamber. Furthermore, we included a

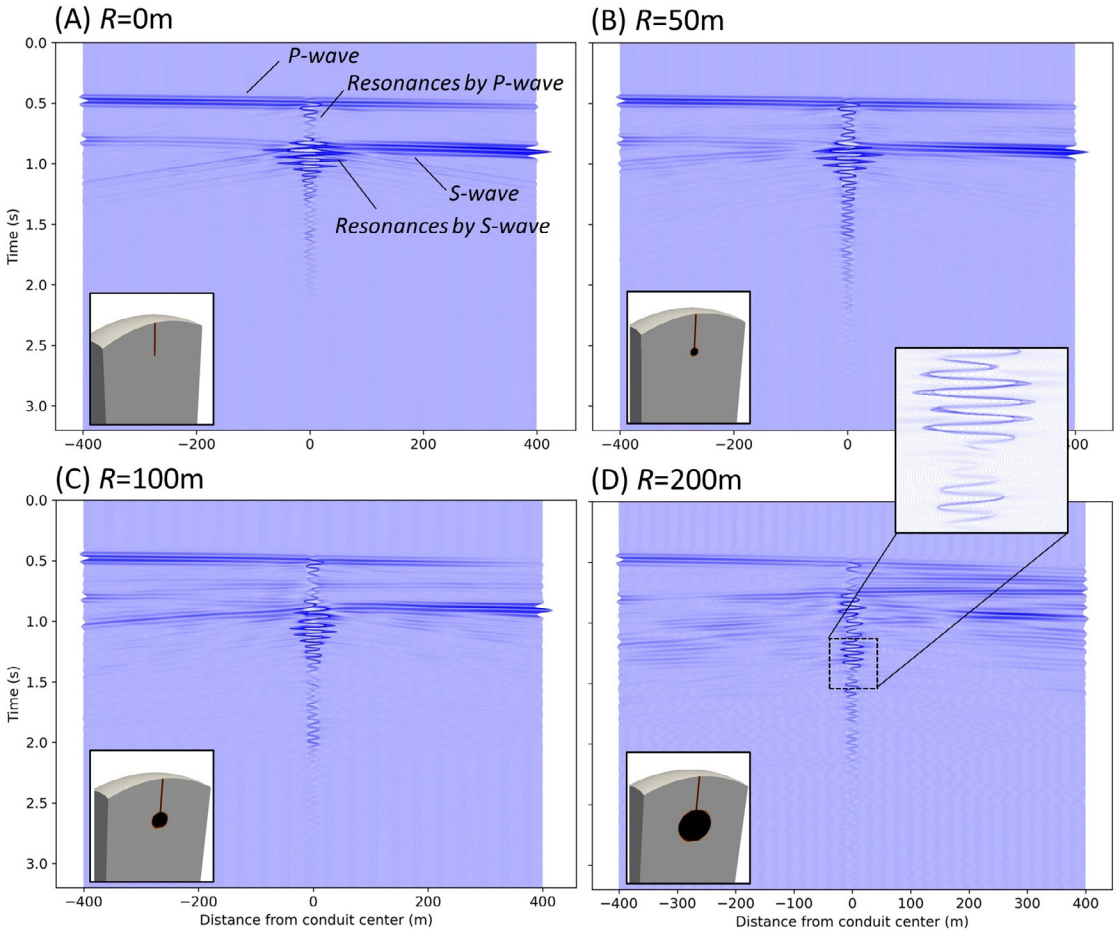

Figure 3: [A]–[D] Synthetic seismograms (*z*-component) obtained from the receiver line across the conduit along the x-axis of the model. Amplitude and duration of the resonances correlate with the increasing size of the magma chamber from R = 0 m to R = 200 m. Long-lasting 'calabash resonances' are most prominent in the immediate vicinity of the conduit. A larger magma chamber leads to a more dispersed scattered wavefield on both sides of the conduit which results from internal reverberations (most notably in [D]). All seismograms are commonly scaled.

local seismic source outside the conduit to simulate a volcanic-tectonic event (see Figure 1).

The results show that resonances, excited by an external seismic source, are significantly influenced by both the width of the conduit and the size of the magma chamber (see Figure 4). The resonant and related scattered wavefields that result from the interaction of the incident waves with the magma chamber-conduit system are observable not just near the conduit, consistent with findings from previous studies [Jousset et al. 2004], but also at more distant seismic stations, several hundred meters away from the center. The amplitudes and frequency characteristics of the 'calabash resonances' (see Figure 2) vary significantly based on the receiver locations (Figure 3, 4). Notably, we detect an amplification of the resonant wavefield towards higher frequencies at receivers positioned close to the conduit, especially when the conduit is narrow and the magma chamber is large (Figure 4).

We studied the physical link between resonance characteristics and wave velocity by systematically decreasing the S-wave velocity in the magma, which in turn means an increase of the Vp/Vs ratio (Figure 5). A significantly decreased S-wave velocity represents a very liquid magma with higher mobility and lower density than a denser and less mobile material, which could be a consequence of a higher proportion of crystals in the magmatic mush, for example. The correlation between seismo-elastic parameters and the overall rheology of the magma was previously explored in laboratory studies, e.g. by Caricchi et al. [2008]. Their research revealed that Vs exhibits an increment with an increase in magma crystallinity. According to these findings, our study underscores the potential utility of seismograms, particularly resonances, recorded at volcanic sites to infer rheological characteristics of the magma within the volcanic edifice.

We further consider the potential effects of modifications to our model assumptions. Relevant figures are provided in the supplementary materials. To account for different incidence angles and scenarios of the wave entering the magmatic structures, we simulated the seismic wavefield for a source positioned above the chamber adjacent to the conduit (Supplementary Material 1 Figure S1). Prolonged reverberations are evident, suggesting that the resonances in our study can occur in various situations: a seismic source below the mag-

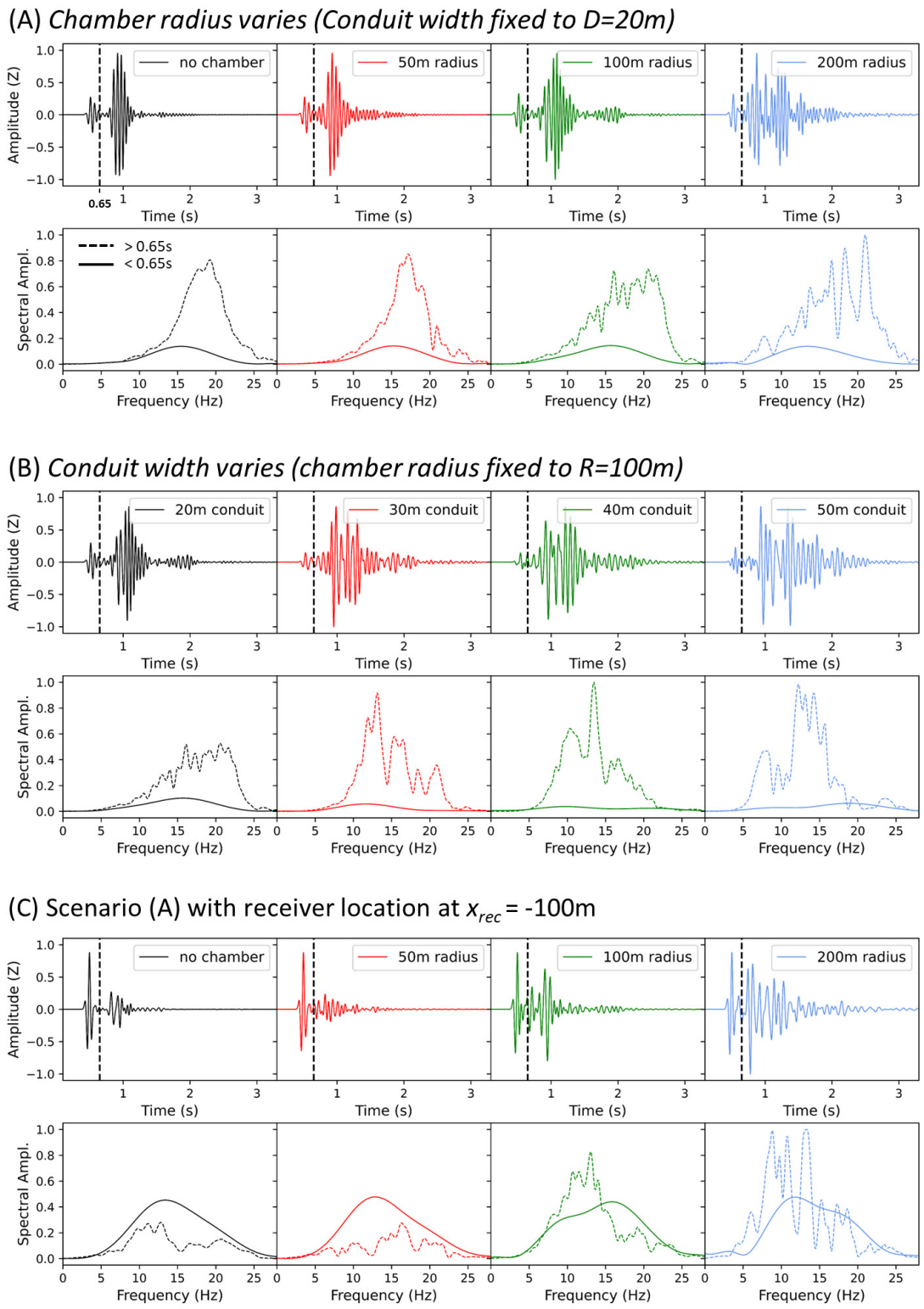

Figure 4: [A] Synthetic seismograms (*z*-components) and spectra for a receiver at the center of the conduit (at x = 0 m) for different magma chamber sizes. The amplitude spectra are calculated separately for times <0.65 s (solid line) and >0.65 s (dashed line) to enhance the resonant wavefields (>0.65 s). [B] Seismograms and spectra at the same position for different widths of the conduit. [B] Seismograms and spectra for a receiver off the center, at x = –100 m, for different sizes of the magma chamber. All waveforms and spectra are commonly scaled to the maximum amplitude within the four waveforms (spectra).

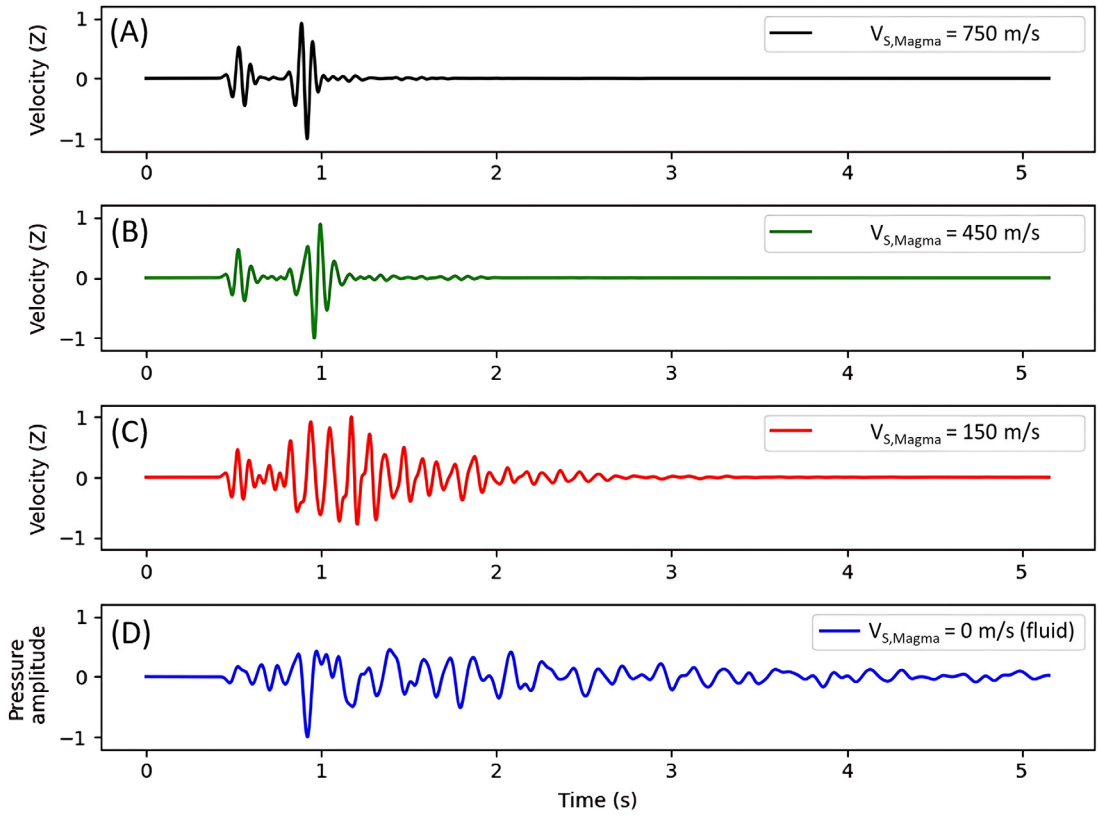

Figure 5: Effect of the ratio between the S-wave velocities of magma and the host rock on the resonances (with receiver located at x = 0 m) for various velocities: [A] $Vs_{,Magma}$ = 750 m s^{-1}, [B] $Vs_{,Magma}$ = 450 m s^{-1}, [C] $Vs_{,Magma}$ = 150 s^{-1}, and [D] $Vs_{,Magma}$ = 0. These are compared to the resonances for an acoustic fluid magma [D]. Due to the numerical limitations of the software utilized, simulations are conducted in 2D, the model does not incorporate a magma chamber, and the conduit width is D = 20 m.

matic structure (Figure 2), next to the conduit (Supplementary Material 1 Figure S1) and a distant earthquake (Figure 6). In general, the wave is refracted and is reflected as it enters the chamber and conduit, as indicated by the wave fronts in the magma chamber in Figure 2 and as shown by prolonged reverberations (e.g. Figure 3). However, our results indicate that the incidence angle is not a key aspect for the generation of resonances. Additionally, we compared seismograms obtained from a receiver line oriented along the y-axis (perpendicular to vertical plane depicted in Figure 2) to those from receivers set along the x-axis. We observed consistent resonances at all receivers (refer to Supplementary Material 1 Figure S2), which illustrates the capability to detect both scattered and resonance wavefields from any direction within the volcanic edifice. Furthermore, we modeled the impact of very high-frequency waves (up to 60 Hz) to investigate the seismic response of structures that are considerably large compared to the length of an incoming wave (Supplementary Material 1 Figure S3). Our findings suggest that these waves may not possess the capability to effectively induce resonances in magmatic structures. This conclusion is primarily attributed to the limited wavelength of these waves in comparison to the dimensions of the structures.

Resonances produced by fluid tubular and spherical inclusions have also been quantified using analytically derived dispersion relationships [e.g. Paillet and White 1982; Schneider et al. 2017]. However, given the combined effects of the chamber-conduit system and the complexities arising from considering both P- and S-waves propagating within the magmatic structures, we assume that the resonant wavefield obtained through the numerical simulations surpasses the constraints of analytical approximations. Consequently, we utilize an idealized structural model comprising a sphere attached to a tube, along with a fixed source frequency and topography. The aim is to emphasize the fundamental wave dynamics of the 'calabash resonances' resulting from the interaction between a wavefield and a magmatic structure. In order to further advance the understanding of this phenomenon, future investigations should explore the effects of more intricate structures situated at various depths. Additionally, forthcoming models ought to incorporate topographic effects and a heterogeneous velocity model to examine the chances and limitations of recording resonances and scattering across the edifice. The comparison between Figure 4A and 4C reveals that the location of the receiver significantly impacts the spectral and temporal characteristics of the seismograms, which can be further influenced by a more complex and detailed surface topography.

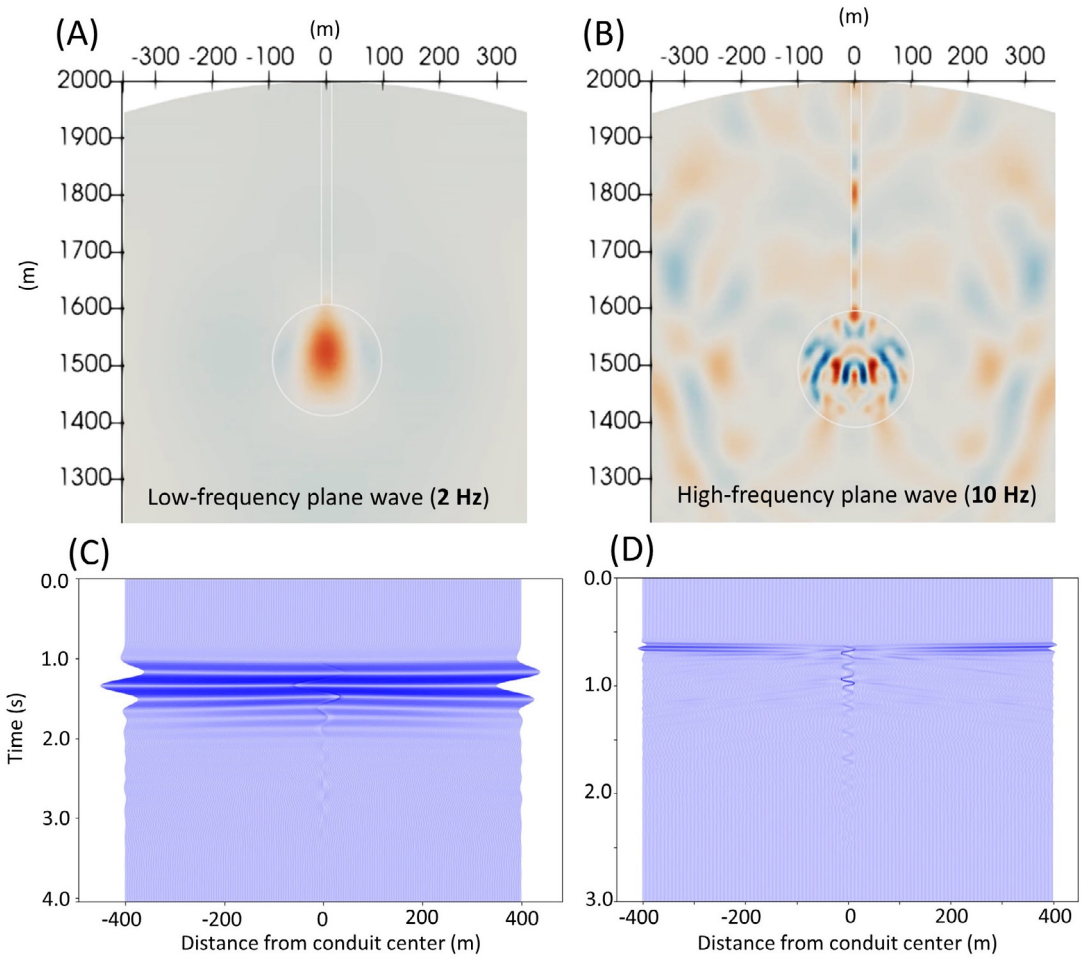

Figure 6: Wavefields and seismograms simulate an incoming plane wave from the bottom of the computational model to approximate a distant earthquake with dominant frequencies of 2 Hz ([A] and [C]) and 10 Hz ([B] and [D]). Corresponding seismic traces ([C] and [D]) reveal that the 2 Hz incoming wavefield does not induce significant resonances, compared to the 10 Hz incoming wavefield. This implies that the resonances depend on the wavelength of the incoming wave. The wave-capturing process is more sufficient in case of a shorter wavelengths that are able to resolve the magmatic structures ([B] and [D]). The vertical axis (horizontal axis) in [A] and [B] represent the vertical z-axis (horizontal x-axis) of the model (Figure 1).

5 Conclusion

This study employs numerical models to simulate seismic resonances in a magma-filled chamber and conduit system when induced by an externally excited wavefield. Our results reveal that the resonances are influenced by multiple factors, including magma chamber size, conduit width, magma rheology, receiver location, and signal frequency.

Central to our findings is the observation that larger magma chambers and wider conduits enhance resonant behavior at the tested frequency. This is evident from the significant splitting in the amplitude spectra. Wide conduits yield lower-frequency resonances, while larger magma chambers generally broaden the spectrum of the seismic response, also towards higher frequencies. Intriguingly, the frequency content of the P-wave remains consistently unaffected by these variations, highlighting the complex interplay between the magma chamber, conduit, and the seismic wavefield. Furthermore, we demonstrate that the characteristics of resonances measured at the volcano's surface correlate systematically with the shear wave velocity in the magma, having the potential to unveil crucial insights to the rheological characteristics of the magma.

By studying the wavefields arising from the combined influence of both the conduit and magma chamber, our numerical results provide important insights into the relationship between waveform characteristics and magmatic structures, especially in scenarios where analytical methods face limitations. We are hopeful that our study will inspire further observational and analytical research to identify and analyze the described 'calabash resonances' in seismic recordings from volcanoes worldwide.

Author Contributions

GR initiated this study. FL built up the model, performed all simulations and processed the synthetic data. FL and GR conceptualized the modeling approach and interpretated the

results. FL wrote the first draft of the manuscript. GR and FL edited and finalized the manuscript.

Acknowledgements

We express our gratitude to Taiyi Wang, Finnigan Illsley-Kemp, and the anonymous referee for their valuable comments and suggestions, which enhanced the quality of this manuscript. We would also like to thank to Chiara Montagna for editorial handling of our submission to Volcanica.

Data Availability

All simulations are performed based on the commercial software package `Salvus` [Afanasiev et al. 2018]. The `Salvus`-script developed for this study can be requested from the corresponding author and are stored in a repository (https://hessenbox-a10.rz.uni-frankfurt.de/getlink/fi63dpx9dCVURuPbQM7iX2/). Additional supplementary figures are available alongside the online version of this article in Supplementary Material 1.

References

Afanasiev, M., C. Boehm, M. van Driel, L. Krischer, M. Rietmann, D. A. May, M. G. Knepley, and A. Fichtner (2018). "Modular and flexible spectral-element waveform modelling in two and three dimensions". *Geophysical Journal International* 216(3), pages 1675–1692. DOI: 10.1093/gji/ggy469.

Cadena, Ó. E. and J. J. Sánchez (2022). "Conduit resonance models for long-period seismicity at Galeras volcano (Colombia), during 2004–2010". *Journal of South American Earth Sciences* 113, page 103661. DOI: 10.1016/j.jsames.2021.103661.

Caricchi, L., L. Burlini, and P. Ulmer (2008). "Propagation of P and S-waves in magmas with different crystal contents: Insights into the crystallinity of magmatic reservoirs". *Journal of Volcanology and Geothermal Research* 178(4), pages 740–750. DOI: 10.1016/j.jvolgeores.2008.09.006.

Chouet, B. (1986). "Dynamics of a fluid-driven crack in three dimensions by the finite difference method". *Journal of Geophysical Research: Solid Earth* 91(B14), pages 13967–13992. DOI: 10.1029/jb091ib14p13967.

– (1988). "Resonance of a fluid-driven crack: Radiation properties and implications for the source of long-period events and harmonic tremor". *Journal of Geophysical Research: Solid Earth* 93(B5), pages 4375–4400. DOI: 10.1029/jb093ib05p04375.

Christensen, N. I. and D. Stanley (2003). "83 Seismic velocities and densities of rocks". *International Handbook of Earthquake and Engineering Seismology*. Elsevier, pages 1587–1594. DOI: 10.1016/s0074-6142(03)80278-4.

De Barros, L., C. J. Bean, M. Zecevic, F. Brenguier, and A. Peltier (2013). "Eruptive fracture location forecasts from high-frequency events on Piton de la Fournaise Volcano". *Geophysical Research Letters* 40(17), pages 4599–4603. DOI: 10.1002/grl.50890.

De Siena, L., C. Thomas, G. P. Waite, S. C. Moran, and S. Klemme (2014). "Attenuation and scattering tomography of the deep plumbing system of Mount St. Helens". *Journal of Geophysical Research: Solid Earth* 119(11), pages 8223–8238. DOI: 10.1002/2014jb011372.

Domínguez, T., V. M. Zobin, and G. A. Reyes-Davila (2001). "The fracturing in volcanic edifice before an eruption: the June–July 1998 high-frequency earthquake swarm at Volcán de Colima, México". *Journal of Volcanology and Geothermal Research* 105(1–2), pages 65–75. DOI: 10.1016/s0377-0273(00)00243-2.

Ferrazzini, V. and K. Aki (1987). "Slow waves trapped in a fluid-filled infinite crack: Implication for volcanic tremor". *Journal of Geophysical Research: Solid Earth* 92(B9), pages 9215–9223. DOI: 10.1029/jb092ib09p09215.

Gómez M, D. M. and R. A. Torres C (1997). "Unusual low-frequency volcanic seismic events with slowly decaying coda waves observed at Galeras and other volcanoes". *Journal of Volcanology and Geothermal Research* 77(1–4), pages 173–193. DOI: 10.1016/s0377-0273(96)00093-5.

Hagerty, M., S. Schwartz, M. Garcés, and M. Protti (2000). "Analysis of seismic and acoustic observations at Arenal Volcano, Costa Rica, 1995–1997". *Journal of Volcanology and Geothermal Research* 101(1–2), pages 27–65. DOI: 10.1016/s0377-0273(00)00162-1.

Helluweg, M. (2000). "Physical models for the source of Lascar's harmonic tremor". *Journal of Volcanology and Geothermal Research* 101(1–2), pages 183–198. DOI: 10.1016/s0377-0273(00)00163-3.

Ji, S., Q. Wang, and L. Li (2019). "Seismic velocities, Poisson's ratios and potential auxetic behavior of volcanic rocks". *Tectonophysics* 766, pages 270–282. DOI: 10.1016/j.tecto.2019.06.013.

Johnson, J. and J. Lees (2000). "Plugs and chugs—seismic and acoustic observations of degassing explosions at Karymsky, Russia and Sangay, Ecuador". *Journal of Volcanology and Geothermal Research* 101(1–2), pages 67–82. DOI: 10.1016/s0377-0273(00)00164-5.

Jousset, P., J. Neuberg, and A. Jolly (2004). "Modelling low-frequency volcanic earthquakes in a viscoelastic medium with topography". *Geophysical Journal International* 159(2), pages 776–802. DOI: 10.1111/j.1365-246x.2004.02411.x.

Jousset, P., J. Neuberg, and S. Sturton (2003). "Modelling the time-dependent frequency content of low-frequency volcanic earthquakes". *Journal of Volcanology and Geothermal Research* 128(1–3), pages 201–223. DOI: 10.1016/s0377-0273(03)00255-5.

Karlstrom, L. and E. M. Dunham (2016). "Excitation and resonance of acoustic-gravity waves in a column of stratified, bubbly magma". *Journal of Fluid Mechanics* 797, pages 431–470. DOI: 10.1017/jfm.2016.257.

Lesage, P., M. J. Heap, and A. Kushnir (2018). "A generic model for the shallow velocity structure of volcanoes". *Journal of Volcanology and Geothermal Research* 356, pages 114–126. DOI: 10.1016/j.jvolgeores.2018.03.003.

Liang, C., L. Karlstrom, and E. M. Dunham (2020). "Magma Oscillations in a Conduit-Reservoir System, Application to Very Long Period (VLP) Seismicity at Basaltic Volcanoes: 1. Theory". *Journal of Geophysical Research: Solid Earth* 125(1). DOI: 10.1029/2019jb017437.

Miller, A. D., R. C. Stewart, R. A. White, R. Luckett, B. J. Baptie, W. P. Aspinall, J. L. Latchman, L. L. Lynch, and B. Voight (1998). "Seismicity associated with dome growth and collapse at the Soufriere Hills Volcano, Montserrat". *Geophysical Research Letters* 25(18), pages 3401–3404. DOI: 10.1029/98gl01778.

Muñoz, F. C., A. E. Nieto, and H. Meyer (1990). "Analysis of swarms of high-frequency seismic events at Nevado del Ruiz volcano, Colombia (January 1986–August 1987): Development of a procedure". *Journal of Volcanology and Geothermal Research* 41(1–4), pages 327–354. DOI: 10.1016/0377-0273(90)90095-w.

Neuberg, J., H. Tuffen, L. Collier, D. Green, T. Powell, and D. Dingwell (2006). "The trigger mechanism of low-frequency earthquakes on Montserrat". *Journal of Volcanology and Geothermal Research* 153(1–2), pages 37–50. DOI: 10.1016/j.jvolgeores.2005.08.008.

Nishi, Y., S. Sherburn, B. J. Scott, and M. Sugihara (1996). "High-frequency earthquakes at White Island volcano, New Zealand: insights into the shallow structure of a volcano-hydrothermal system". *Journal of Volcanology and Geothermal Research* 72(3–4), pages 183–197. DOI: 10.1016/0377-0273(96)00005-4.

O'Brien, G. S., C. J. Bean, H. Meiland, and P. Witte (2023). "Imaging and seismic modelling inside volcanoes using machine learning". *Scientific Reports* 13(1). DOI: 10.1038/s41598-023-27738-6.

Paillet, F. L. and J. E. White (1982). "Acoustic modes of propagation in the borehole and their relationship to rock properties". *Geophysics* 47(8), pages 1215–1228. DOI: 10.1190/1.1441384.

Patanè, D., G. Barberi, P. De Gori, O. Cocina, L. Zuccarello, A. Garcia-Yeguas, M. Castellano, A. D'Alessandro, and T. Sgroi (2017). "The shallow magma chamber of Stromboli Volcano (Italy)". *Geophysical Research Letters* 44(13), pages 6589–6596. DOI: 10.1002/2017gl073008.

Paulatto, M., E. E. E. Hooft, K. Chrapkiewicz, B. Heath, D. R. Toomey, and J. V. Morgan (2022). "Advances in seismic imaging of magma and crystal mush". *Frontiers in Earth Science* 10. DOI: 10.3389/feart.2022.970131.

Power, J. A., J. C. Lahr, R. A. Page, B. A. Chouet, C. D. Stephens, D. H. Harlow, T. L. Murray, and J. N. Davies (1994). "Seismic evolution of the 1989–1990 eruption sequence of Redoubt Volcano, Alaska". *Journal of Volcanology and Geothermal Research* 62(1–4), pages 69–94. DOI: 10.1016/0377-0273(94)90029-9.

Reiss, M. C., L. De Siena, and J. D. Muirhead (2022). "The Interconnected Magmatic Plumbing System of the Natron Rift". *Geophysical Research Letters* 49(15). DOI: 10.1029/2022gl098922.

Rowe, C., R. Aster, P. Kyle, R. Dibble, and J. Schlue (2000). "Seismic and acoustic observations at Mount Erebus Volcano, Ross Island, Antarctica, 1994–1998". *Journal of Volcanology and Geothermal Research* 101(1–2), pages 105–128. DOI: 10.1016/s0377-0273(00)00170-0.

Schneider, F., S. Esterhazy, I. Perugia, and G. Bokelmann (2017). "Seismic resonances of spherical acoustic cavities". *Geophysical Prospecting* 65(S1), pages 1–24. DOI: 10.1111/1365-2478.12523.

Sturton, S. and J. Neuberg (2003). "The effects of a decompression on seismic parameter profiles in a gas-charged magma". *Journal of Volcanology and Geothermal Research* 128(1–3), pages 187–199. DOI: 10.1016/s0377-0273(03)00254-3.

– (2006). "The effects of conduit length and acoustic velocity on conduit resonance: Implications for low-frequency events". *Journal of Volcanology and Geothermal Research* 151(4), pages 319–339. DOI: 10.1016/j.jvolgeores.2005.09.009.

Wang, T. A., E. M. Dunham, L. Krenz, L. S. Abrahams, P. Segall, and M. R. Yoder (2024). "Dynamic Rupture Simulations of Caldera Collapse Earthquakes: Effects of Wave Radiation, Magma Viscosity, and Evidence of Complex Nucleation at Kilauea 2018". *Journal of Geophysical Research: Solid Earth* 129(4). DOI: 10.1029/2023jb028280.